La mer 32: 307–324, 1994
Société franco-japonaise d'océanographie, Tokyo

Preliminary evaluation of a Gulf of Mexico circulation model at 92°W

Christopher N. K. MOOERS*, San JIN* and Dong-Shan KO*

Abstract: As part of the U. S. Minerals Management Service (MMS) Gulf of Mexico Modeling Program, the efforts to assess preliminarily the skill of an exploratory application of the BLUMBERG-MELLOR (1983) model to the Gulf of Mexico by OEY and ZHANG (1993) are described. Three years of model output are analyzed and compared to current meter records, typically of one-year duration, along 92°W, allowing demonstration of some of the skill assessment methodology. The model was driven with ocean climatology on its open boundaries, climatological mean winter atmospheric forcing, and climatological mean river runoff from the Mississippi and Atchafalaya Rivers. The salient results of the preliminariy assessment are

—the model output and observed data have comparable mean and rms amplitudes, and generally similar space-time structure
—the model output indicates a strong eastward jet at the shelfbreak, which is also the locus of high variability, requiring further observational confirmation
—the eddy passages apparently impact substantially the shelfbreak region
—the shelfbreak region, due to its concentration of mean flow and variability (and presumably shelf-Gulf of Mexico exchange), must be accounted for in designing model and observational domains and grids for the LATEX (Louisiana-Texas shelf) region.

1. Introduction

As numerical circulation models for marginal and semi-enclosed seas are under rapid development, it is important to begin to evaluate them thoroughly relative to observations. Realizing that there are parallels to be drawn between the circulation of the Gulf of Mexico and the circulation of the East Asian Seas, especially the Sea of Japan, this paper illustrates a contemporary effort in the USA to evaluate a numerical circulation model relative to observations in the Gulf of Mexico. Hopefully, future works in evaluating numerical circulation models for the East Asian Seas will be stimulated by the present paper, and will lead to comparisons with Gulf of Mexico circulation models.

A preliminary skill assessment of a Gulf of Mexico circulation model is made by comparing model output to observations from a moored current meter array deployed over the continental shelf and slope along 92°W. (This assessment is preliminary in the sense that soon a more advanced version of the model from Dynalysis of Princeton, and more complete observations from the Louisiana-Texas Shelf Physical Oceanography Program (LATEX) field program will be available for skill assessment.) The objectives are (1) to seek a preliminary validation of the model, (2) to examine model design issues associated with shelfbreak variability and exchange processes, and (3) to demonstrate several skill assessment methodologies.

The Gulf of Mexico circulation model utilized is the BLUMBERG-MELLOR (often known as the Princeton Ocean Model) sigma coordinate, primitive equation model (BLUMBERG and MELLOR, 1983) implemented on a ca. 20km rectangular grid (and with 21 sigma levels) by OEY and ZHANG (1993). The model was initialized with hydrographic climatology (LEVITUS, 1982), and it was driven by climatological mean winter wind forcing (HELLERMAN and ROSENSTEIN, 1983), climatological mean winter surface heat and evaporative fluxes (from Surface

* Ocean Prediction Experimental Laboratory, Rosenstiel School of Marine and Atmospheric Science, University of Miami, 4600 Rickenbacker Causeway, Miami, Florida 33149-1098, U.S.A.

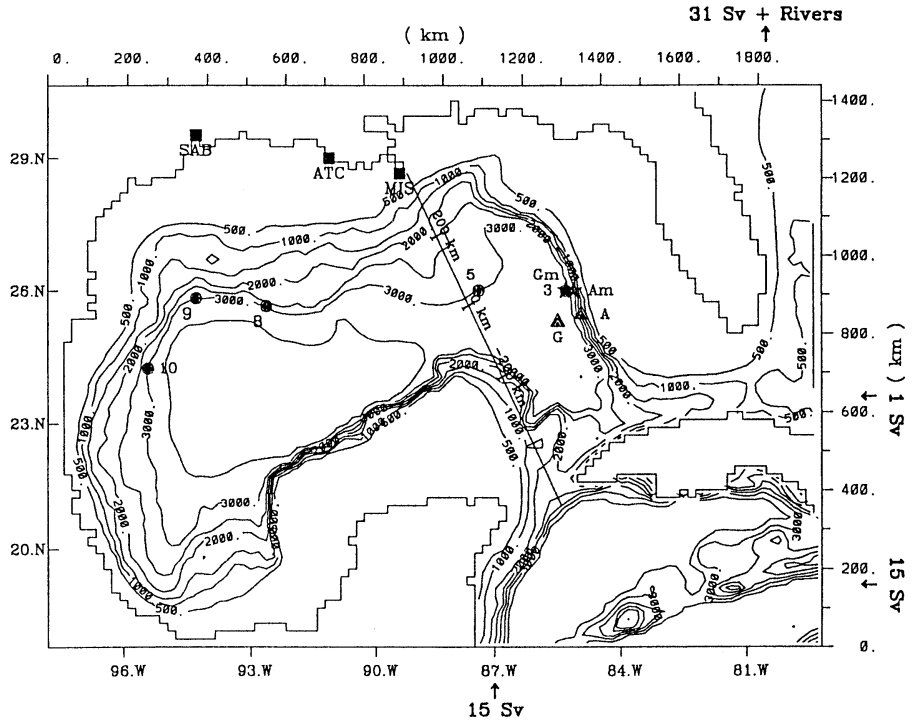

Fig. 1. Gulf of Mexico model domain. Isobaths are in meters; squares indicate river discharge points: MIS – Mississippi, ATC–Atchafalaya, SAB–Sabine.

Marine Observations data set, National Climate Data Center) and mean river runoff (based on stream gauge data from the U.S.Army Corps of Engineers, W. WISEMAN, Louisiana State Univ., personal communications); the model was also relaxed to climatological winter surface temperature and salinity (LEVITUS, 1982); see OEY and ZHANG (1993) for more details. Thus, neither tidal nor synoptic (or seasonal) wind and thermohaline forcing were applied to the model. Three years of five-day averaged model output data were analyzed from year four-to-seven of the model simulation, i.e., after the model had spun-up (based on the realistic broadband frequency of Loop Current eddy-shedding exhibited by the model). Since the forcing was not time-specific, only statistical comparisons between model and observations can be performed, i.e., phase comparisons are meaningless.

The moored current meter array had been deployed along 92°W from 1987 through 1989 by Science Applications Incorporated (SAIC) (sponsored by the Mineral Managements Service). (Analyses of some of these and additional data have been provided by HAMILTON (1990, 1992).) There were 29 current meters mounted on seven moorings. The sampling rate was half-hourly. The maximum common record length of credible data for several current meters was about one year. The focus in this paper is on one current meter mooring (upper-slope station) located near the shelfbreak; data from the outer-shelf station are introduced where essential.

Hence, the model output lacked the realism afforded by synoptic or seasonal atmospheric, seasonal runoff, and tidal forcing. Furthermore, the current meter data were limited in horizontal and vertical resolution, record durations, and temporal continuity. One consequence is that no seasonality can be inferred in the comparisons and interpretations, only gross comparisons and interpretations. A more fine-grained analysis will become possible when more realistic forcing is applied to the more advanced model, and when more comprehensive observational data sets are available. However, the

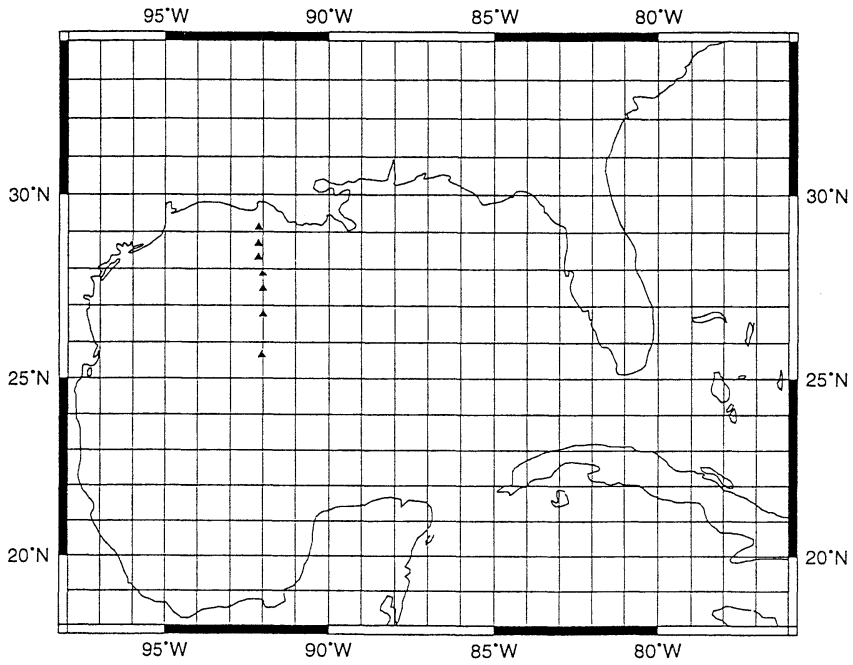

Fig. 2. Location of current meter mooring along 92°W. Triangles indicate moorings.

model was sufficiently realistic, and the observed data were sufficiently complete, to enable a worthwhile preliminary skill assessment of the model. In turn, this preliminary skill assessment allows demonstrating some of the skill assessment methodology developed under the Gulf of Mexico Modeling Program.

2. Background

This preliminary skill assessment has been performed, in part, to assess the results of OEY and ZHANG (1993), and, in part, to develop, test, and demonstrate some of the methods useful in model evaluation. The focus here is on the use of kinematical and statistical comparisons. Due to data availability, the emphasis is placed on time series comparisons at a specific location, vertical section analyses, and cross-shore transect analyses. There is an entire additional class of analyses to be applied to horizontal (2–D) data sets and 3–D data sets that will be possible when LATEX data become available.

Model and observational configurations. The model domain covers the Gulf of Mexico, Straits of Florida, and the northwest Caribbean Sea (Fig.1). The bottom topography is a smoothed version of DBDB5 (National Geophysical Data Center, 1986) and includes the continental shelves and quite realistic representations of major topographic features. The moored current meter array along 92°W (Fig. 2) extends from nearshore to the central Gulf.

The model is driven by the constant wind, heat, and runoff forcing mentioned above, plus specified (constant) inflows (a total of 30 Sv based on the Levitus climatology) along the southern and eastern boundaries in the Caribbean Sea, so that the model can organize its own Yucatan Current, which is not necessarily steady in time, and 1 Sv through the Bahama Islands. The model develops a Loop Current which aperiodically sheds anticyclonic eddies (Fig. 3; from OEY and ZHANG, 1993). These eddies subsequently propagate to the western Gulf and impinge upon the continental margin off Texas and Mexico (Fig. 4; from OEY and ZHANG, 1993). The mean eddy propagation path of eight model eddies falls within the envelope of observed (by satellite IR imagery from VUKOVICH at SAIC) decadal-mean trajectories (not shown). This qualitative agreement suggests that it would be

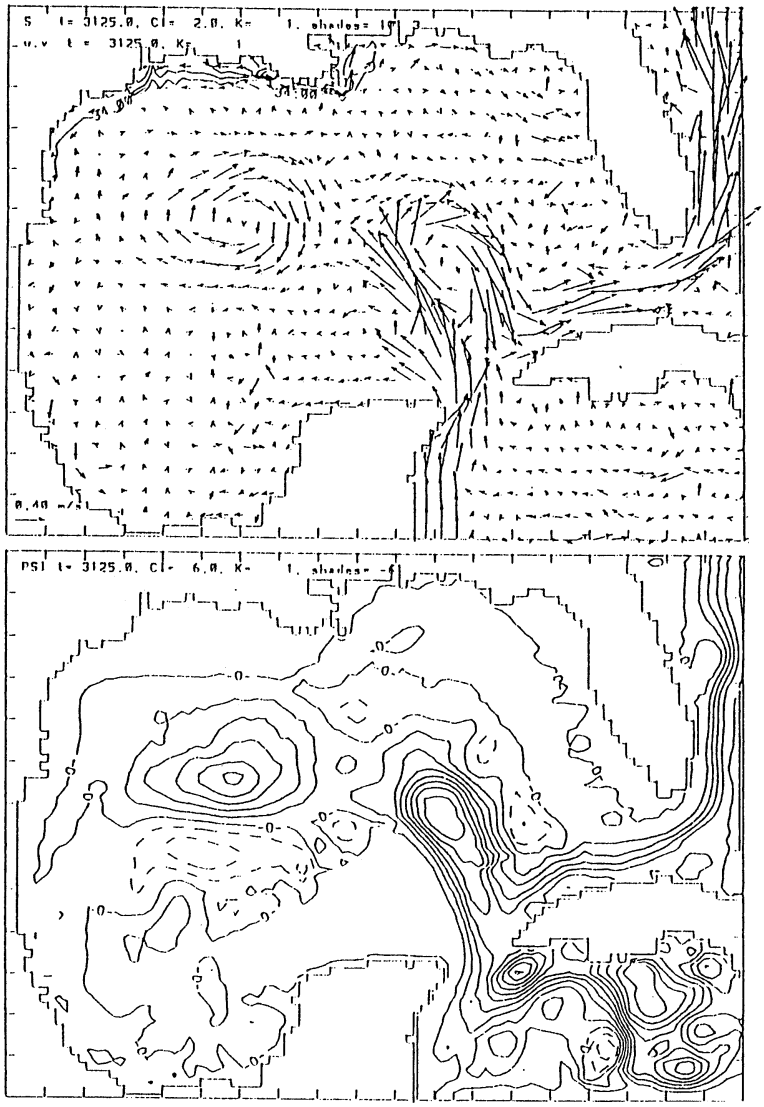

Fig. 3. Model output (OEY and ZHANG, 1993). Upper: synoptic surface currents at model day 3152, lower: corresponding synoptic total stream function (contour interval: 6 Sverdrups).

worthwhile to examine further the level of realism in the model output.

The model's sigma coordinate and rectangular grid system (Fig. 5) is intended to provide horizontal and vertical resolution adequate to describe the Loop Current, its eddy-shedding, and the eddy propagation and decay in the open Gulf. It is also intended to provide vertical resolution adequate to resolve wind-driven and buoyancy-driven transient circulation over the continental shelf and slope. The design of the moored current meter array had similar objectives over the continental margin. In particular, the moored array had three elements between the mid-shelf and upper-slope (Fig. 5), spanning a distance of ca. 100 km. Each of these moorings had typically three-to-four current meters on any one deployment.

For the purposes of this preliminary assessment, the analysis will focus on one station near the shelfbreak: the upper-slope station at 27.88°N in a water depth of 210m. For compari-

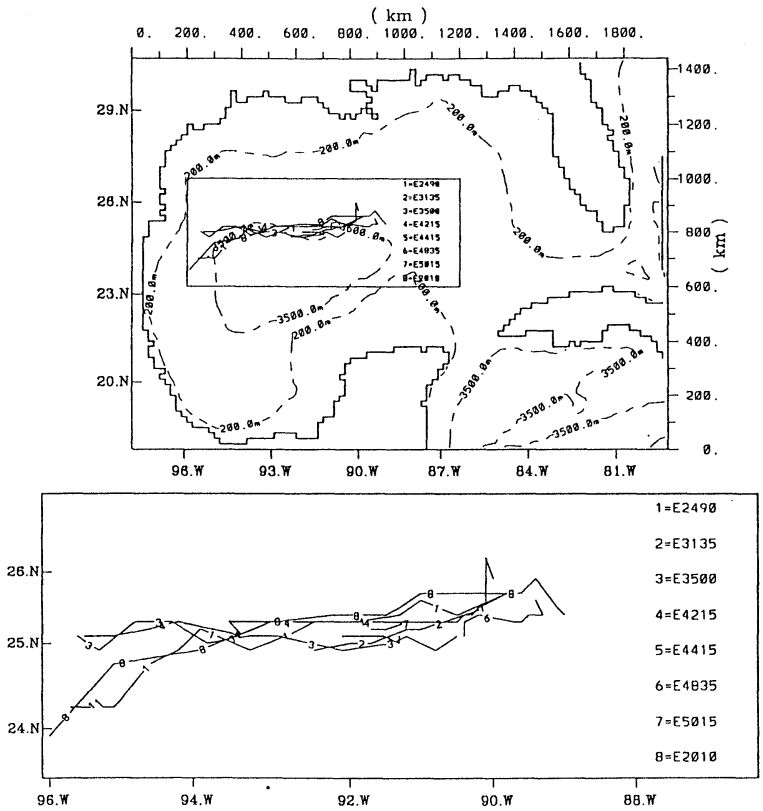

Fig. 4. Loop Current spin-off anticyclonic eddy trajectories. Upper: eight model eddy trajectories (solid lines), lower: the eight model eddy trajectories at expanded scale.

son with the observations, model output was chosen at the grid point whose water depth was closest to that of the observational station water depth. In particular, the upper-slope station is compared to model output at the grid point at 27.89°N in a water depth of 217m.

The time-continuity of the observational data is somewhat problematic. For example, at the upper-slope station (Fig. 6), there were records (with small gaps) at the upper levels for the majority of 1987 and 1988, while there was nearly a two-year record at the mid-levels, but the record length was less than a year at the lower level.

3. Overview of model output along 92°W

To demonstrate the character, structure, and spatial scales of variability in the model output, the mean and standard deviation fields are examined along 92°W (Fig. 7). Ideally, there would be sufficient observational data to evaluate these fields comprehensively. However, that is not the case, yet these model output fields provide a perspective for the preliminary assessment.

The zonal (along-shore) flow (Fig. 7a) is dominated by a mean eastward jet (with speeds up to 30 cms^{-1}) located over the shelfbreak (between ca. 50 and 1200m isobaths) and confined to the upper 800m. There is a maximum (up to 6 cms^{-1}) in the rms zonal velocity co-located with the shelfbreak jet. A secondary feature is the pair of mean inner-shelf (water depth of 15 to 30m), nearsurface (upper 10m) westward jets (up to 20 cms^{-1}). The mean westward flow nearshore is consistent with the buoyant coastal jets anticipated from the discharges of the Mississippi and Atchafalaya Rivers. The mean eastward flow over the shelfbreak region is qualitatively consistent with the return flow inferred from hydrography by COCHRANE and KELLY (1986).

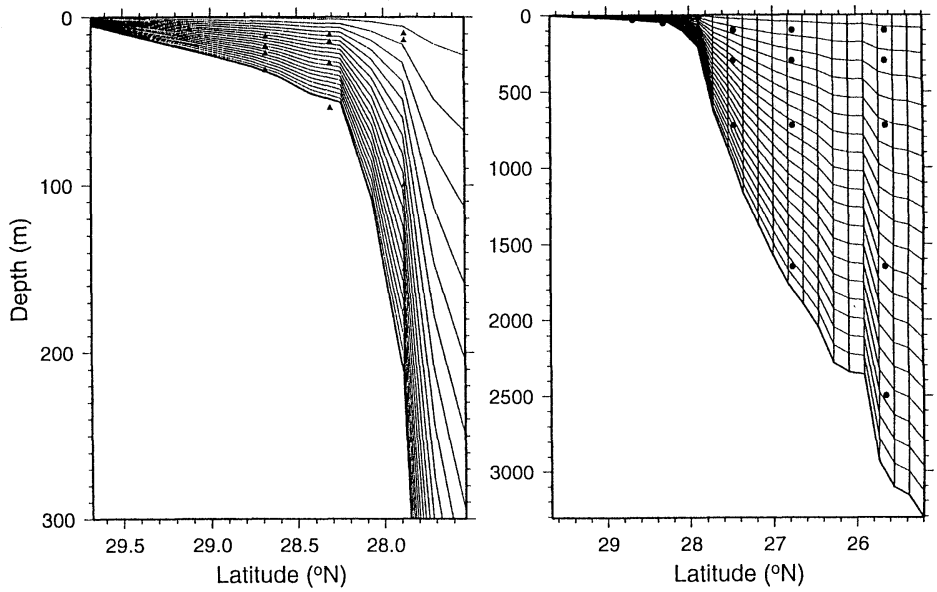

Fig. 5. Model grid and current meter positions along 92°W. Left: expanded shelf domain; right: full coastal ocean domain. Solid triangles and circles indicate current meter locations.

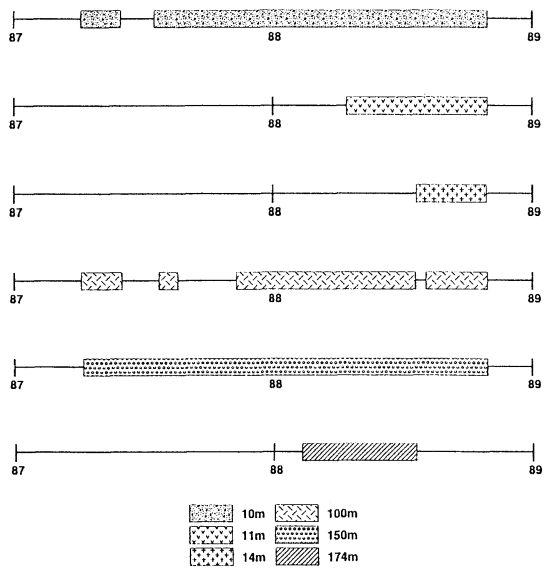

Fig. 6. Time-line of current meter data along 92°W. Upper-slope station (27.9°N; 210m water depth)

Over the inner-shelf, the meridional (cross-shore) flow (Fig. 7b) is dominated by mean nearsurface onshore flow and nearbottom onshore flow, which are consistent (in an Ekman sense) with the applied westward wind stress and predominant nearbottom eastward flow, respectively. A secondary feature consists of a subsurface divergent mean flow (ca. ± 2 cms^{-1}) over a domain of 100km zonally by 1,000m vertically over the continental slope. The rms meridional velocity has maxima (ca. 3 cms^{-1}) over the outer-shelf, upper-slope, and in the upper 500m at 300 km from the shelfbreak.

The vertical velocity (Fig. 7c) is dominated by mean strong, alternating upwelling and downwelling cells in the lower half of the water column over the lower and upper continental slope, seemingly in association with steep topography. The rms vertical velocity field follows closely the general pattern of the rms meridional velocity field. The vertical velocity field is a prime example of a field which is difficult to observe and independently validate, and, hence, if the model can be otherwise validated, this model field would be valuable for many purposes; e.g., ocean dynamical, water quality, and marine ecosystems studies.

The mean temperature field (Fig. 7d) is dominated by the permanent thermocline and baroclinicity over the continental slope. A secondary feature is the inner-shelf frontal zone (cool water nearshore). The rms temperature field has maxima (ca. 1.2°C) nearbottom over

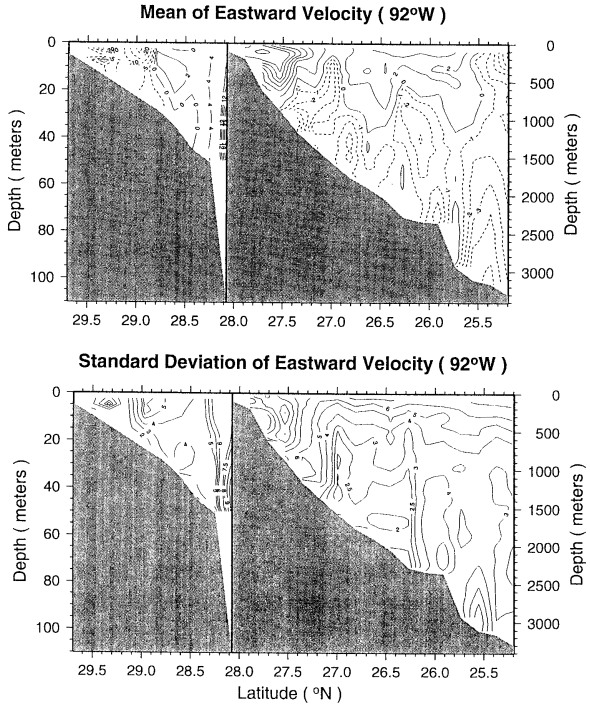

(a) Zonal velocity (u) (positive east; cms^{-1})

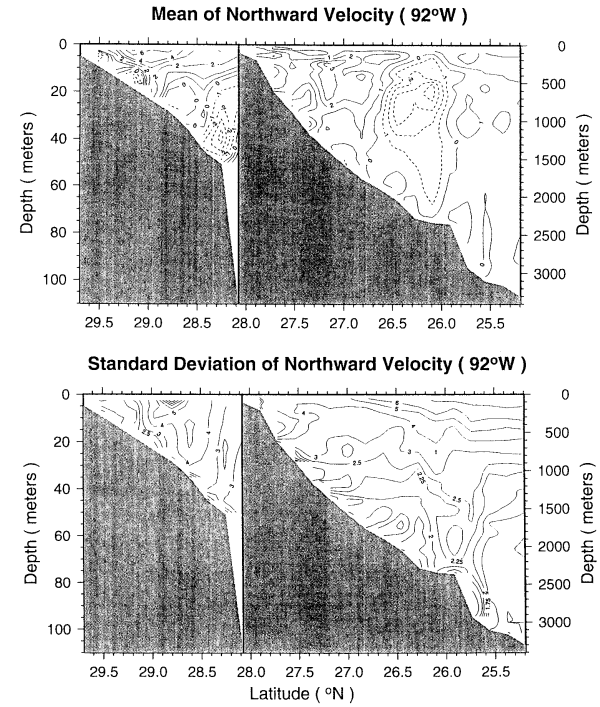

(b) Meridional velocity (v) (positive north; cms^{-1})

Fig. 7. 92°W mean and rms transects for model output. Left: expanded shelf domain; right: full coastal ocean domain.

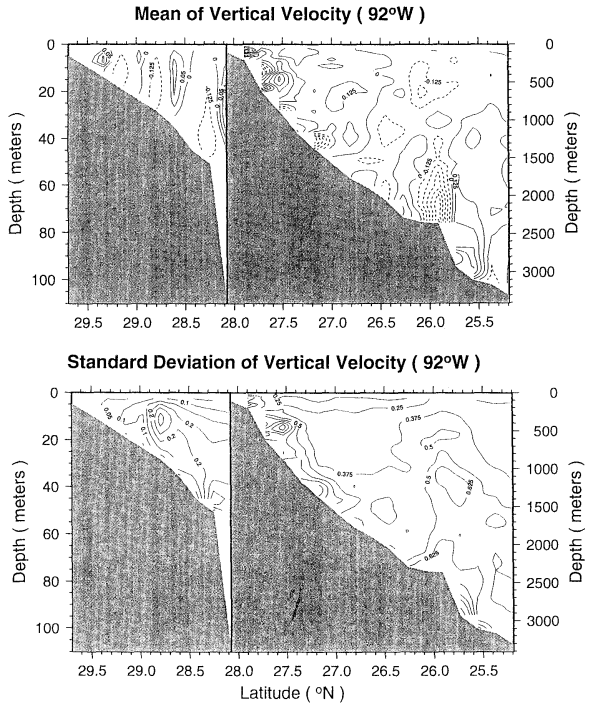

(c) Vertical velocity (w) (positive up; cms^{-1})

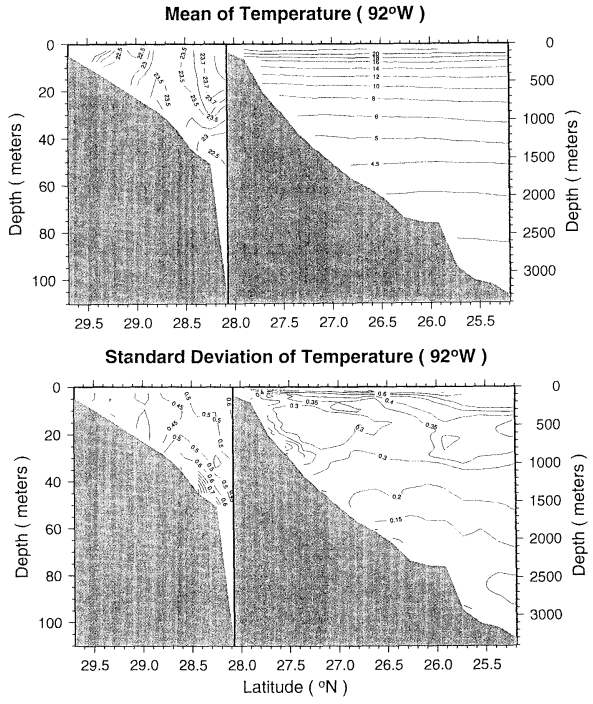

(d) Temperature (T; ˚C)

Fig. 7. 92˚W mean and rms transects for model output. Left: expanded shelf domain; right: full coastal ocean domain.

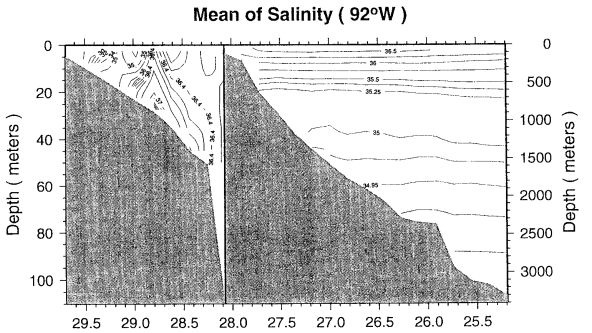

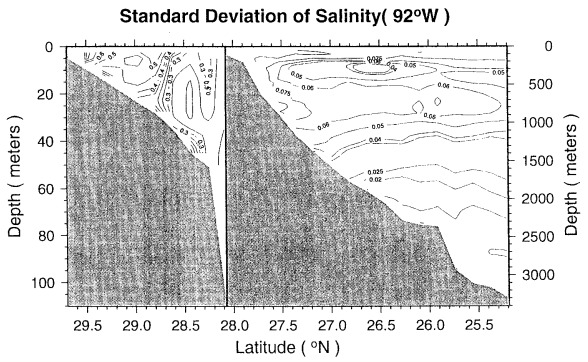

(e) Salinity (ppt)

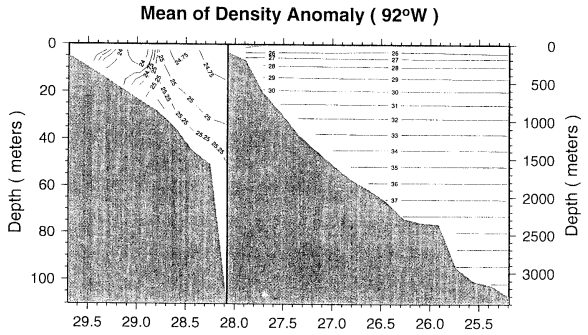

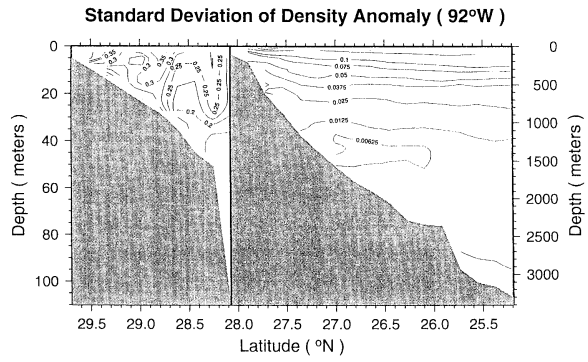

(f) Density (σ_t)

Fig. 7. 92°W mean and rms transects for model output. Left: expanded shelf domain; right: full coastal ocean domain.

the outer-shelf, consistent with transient bottom Ekman flow, and nearsurface (upper 200m) over the continental slope (on the scale of 200km), consistent with eddy passages. The mean salinity field (Fig. 7e) is dominated by a permanent halocline and relatively fresh nearsurface cores over the inner-shelf. The rms salinity field has maxima over the inner-shelf. The mean density field (Fig. 7f) is dominated by the permanent pycnocline, baroclinicity over the slope, and two nearsurface, inner-shelf buoyant cores. The nearshore mean structure of the temperature, salinity and density fields is consistent with the presence of the buoyant coastal jets derived from the Mississippi and Atchafalaya Rivers. The corresponding nearshore rms maxima suggest these jets are highly variable.

Overall, the mean and rms fields appear plausible given what is known of the general circulation in this region; e. g., westward flow along the inner-shelf and return flow over the outer-shelf and slope (COCHRANE and KELLY, 1986). Since the model is driven by mean and not synoptic wintertime atmospheric forcing, it is unable to provide vertical homogenization of the mass field characteristic of the shelf regime during winter (NOWLIN and PARKER, 1974). A most prominent feature is the eastward jet at the shelfbreak which needs independent confirmation and validation. In particular, based on the material presented here, it is unclear whether the jet is attributable to the wind-driven circulation, buoyancy-driven circulation, eddy-induced Reynolds stresses, or the model artifact due to steep topography. With the result from the full ten-year run, OEY and ZHANG (1993) found that the jet was not permanent and was, thus, attributable to eddy passages during the three-year period treated here.

4. Model output-observation data comparisons near the shelfbreak

Comparisons are made of time series, vertical profiles, and spectra at the upper-slope station. The raw half-hourly observations were filtered with a half-power frequency of 5.8 cpd to remove high-frequency internal waves and observational noise, and subsampled to three-hourly values for autospectrum analyses (Fig.12). The three-hourly subsampled observations were then filtered with a half-power frequency of 0.14 cpd to remove tidal and inertial motions, and subsampled to five-day values (to be commensurate with the model output) for time series plots, vertical profile means, standard deviations, and choerence analyses (Fig. 13).

Time domain comparisons. Time series of the zonal (along-shore) velocity (Fig. 8a), meridional (cross-shore) velocity (Fig. 8b), and temperature (Fig. 8c) for three levels at the upper-slope station indicate, most fundamentally, that the current meter and model output data have a common range of values. Since the time axis for the model output has no absolute meaning relative to the time axis of observations (due to the steady forcing applied to the model), the origin of the model output time axis has been adjusted to maximize the overall visual correlation of the zonal and meridional velocities. The major events seen in each are associated with anticyclonic eddy passages, as determined independently from the analysis of surface topography and current maps. The time series of the surface velocity at 92° W versus latitude (Fig. 9) demonstrates eddy passages, as well as the continuous (though variable) nearshore westward jets and the intermittent eastward jet near the shelfbreak. The model output from days 1560 to 2755 is analyzed statistically. The model output from days 1910 to 2645 in Fig. 9 (0 to 735 in Fig. 8) is compared in time series plots with observations, and the eddy passages centered on days 2210 and 2510 are important features in these comparisons; they correspond to eddies 8 and 1, respectively (Fig. 4). From independent studies of satellite AVHRR imagery and in situ observations, two Loop Current anticyclonic eddies were shed during the period of moored current meter data availability in April to October 1987 and April to May 1988 (Tom BERGER, SAIC, personal communications). Hence, the large observed perturbations in zonal velocity during October 1987 and May 1988 (Fig. 8a) possibly correspond to the passage of these eddies.

The amplitudes (ca. 10 to 20 $cm\,s^{-1}$) of the eddy-related perturbations are similar in the observations and model output, as is the interval (ca. 300 days) between eddy passages. In both

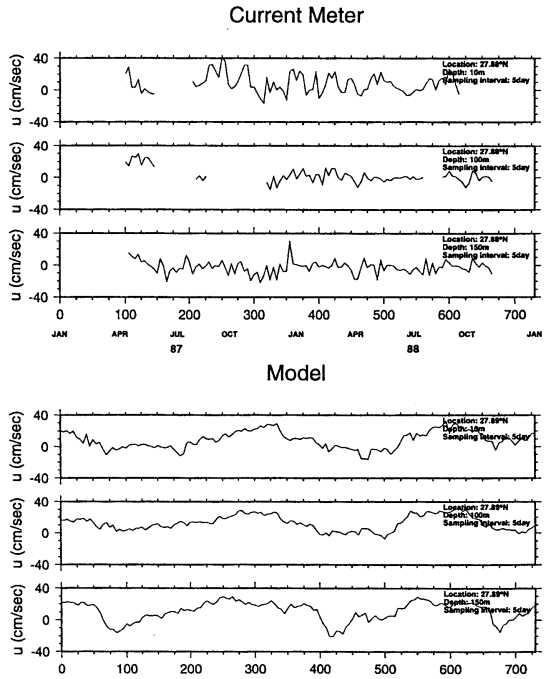

(a) Zonal velocity (u; cm s^{-1}). Upper-slope station (27.9°N; 210m water depth).

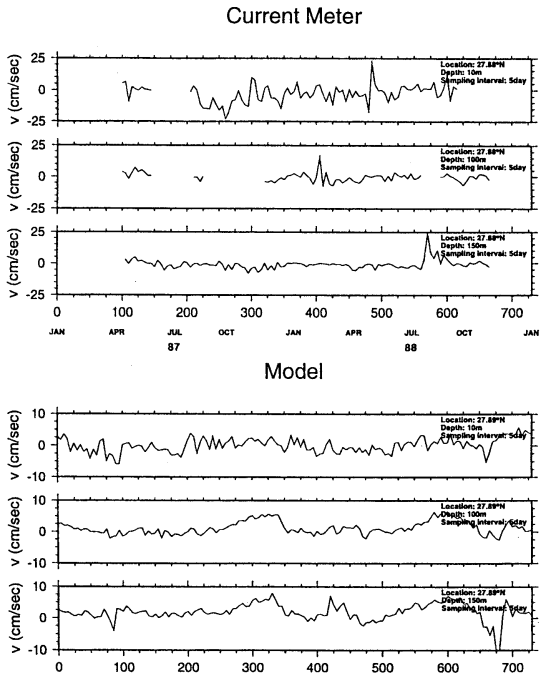

(b) Meridional velocity (v; cm s^{-1}). Upper-slope station (27.9°N; 210m water depth).

Fig. 8. Time series of model output and observed data. Focus is on manifestations of eddy passages at days 300 and 600 near 28°N.

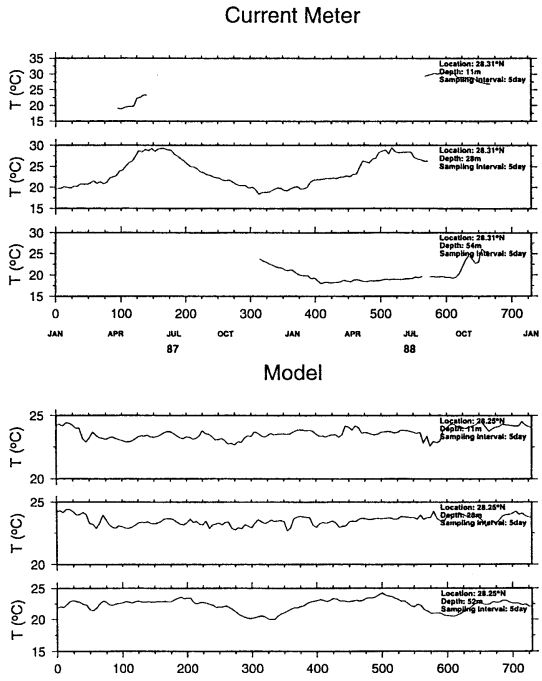

(c) Temperature (T; °C). Upper-slope station (27.9°N; 210m water depth).

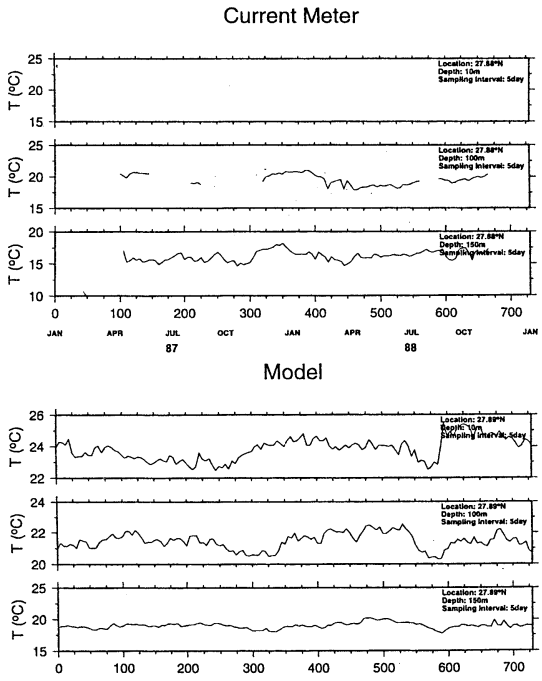

(d) Temperature (T; °C). Outer-shelf station (28.3°N; 60m water depth).

Fig. 8. Time series of model output and observed data. Focus is on manifestations of eddy passages at days 300 and 600 near 28°N.

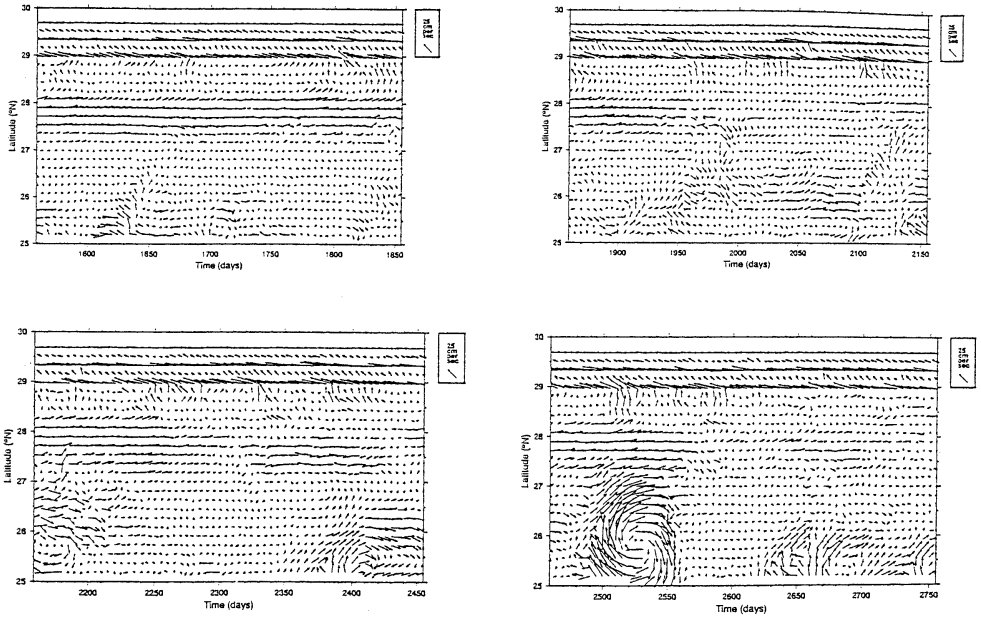

Fig. 9. Time series of model output surface velocity at 92°W versus latitude. Focus is on manifestations of eddy passages at days 2210 and 2510 near 28°N.

the observations and the model output, the large (20 cm s^{-1}) eddy-perturbation zonal velocities are eastward and are confined to the upper water column while the nearbottom perturbations at the outer-shelf station (not shown here) are only a few cm s^{-1}. Not surprisingly, the meridional perturbations are weaker and more variable.

At the upper-slope station (Fig. 8c), there are temperature perturbations of a few degrees associated with eddy passages in the model output. In contrast, the mid-depth temperature observations at the outer-shelf station (Fig. 8d) are dominated by an annual cycle, which, of course, is absent in the model output. There is not an obvious manifestation of the eddy passages in the upper layer temperature of the model output, probably because the eddies barely penetrate to the shelfbreak. However, there is a nearbottom temperature decrease (ca. 2°C) with each eddy passage, probably due to the onshore bottom Ekman transport of cooler water from over the slope.

Vertical profile comparisons. The mean vertical profiles (together with standard deviation bars) calculated from one year of observations and three years of model output are compared (Fig. 10) at the upper-slope station. The mean observed profile is a few cm s^{-1} eastward in the upper half of the water column, but the mean model profile is 10 to 20 cm s^{-1} eastward. The mean profiles of observed and model meridional velocity are similarly weak (1 to 2 cm s^{-1}), but opposite in sign at two of the three observed depths. The mean vertical velocity is upwards in the upper 50 m, downwards between 50 and 125 m, and upwards from 125 to 220 m. The mean model temperature profile is nearly linear with depth, is 4°C cooler than the mean observed temperature nearsurface, and is 2 to 3°C warmer at mid-depths. The model reached a ststistical steady-state by the end of year four, and the next three years of model output have been analyzed here. Hence, these discrepancies in the temperature profiles may reflect flaws in the climatology with which the model was initialized and the artificial thermal forcing applied to the model. (The density profiles are not discussed because they follow from the temperature and salinity profiles.)

The vertical profiles of Reynolds stress for observed and model output data are compared (Fig. 11) at the upper-slope station. The ob-

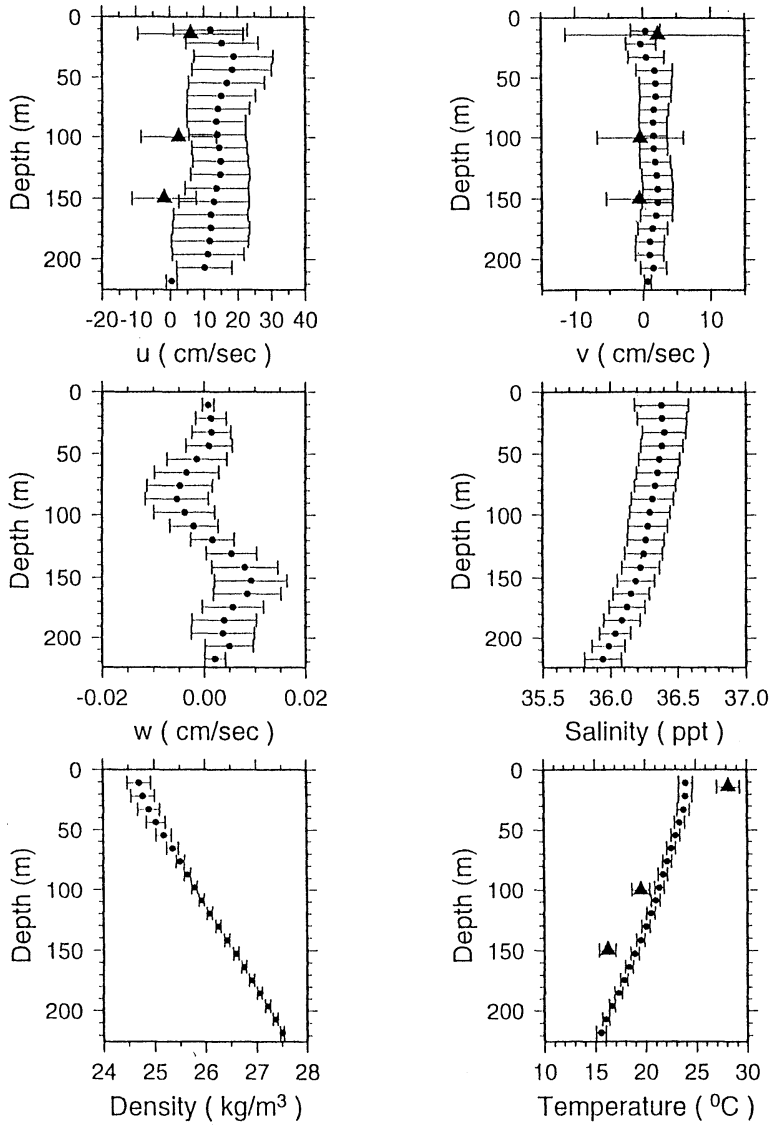

Fig. 10. Mean vertical profiles of model output (solid dots) and observed data (solid triangles) and plus/minus standard deviation bars. Upper-slope station (27.9°N; 210m water depth) (density in σ_t).

served and model values for ⟨u'u'⟩, ⟨v'v'⟩, and ⟨u'v'⟩ agree in order of magnitude. The u', etc. notation is applied to deviations from the record mean.). In contrast, the observed values are generally much greater than the model values for ⟨T'T'⟩, probably due to annual cycle fluctuations in the observations. (Note: temperature was not successfully observed at the upper current meters; thus, these values are missing for ⟨T'T'⟩, etc.) Observed and model values for ⟨u'u'⟩ have double maxima, and for ⟨v'v'⟩ they are generally near zero, except nearsurface for the observed value. Some of the discrepancies in Reynolds stresses may be due to the lack of synoptic atmospheric forcing (especially the manifestations of wintertime cold front passages) applied to the model.

Overall, the mean profiles are generally similar in magnitude and structure, though the eastward jet is much stronger in the model output

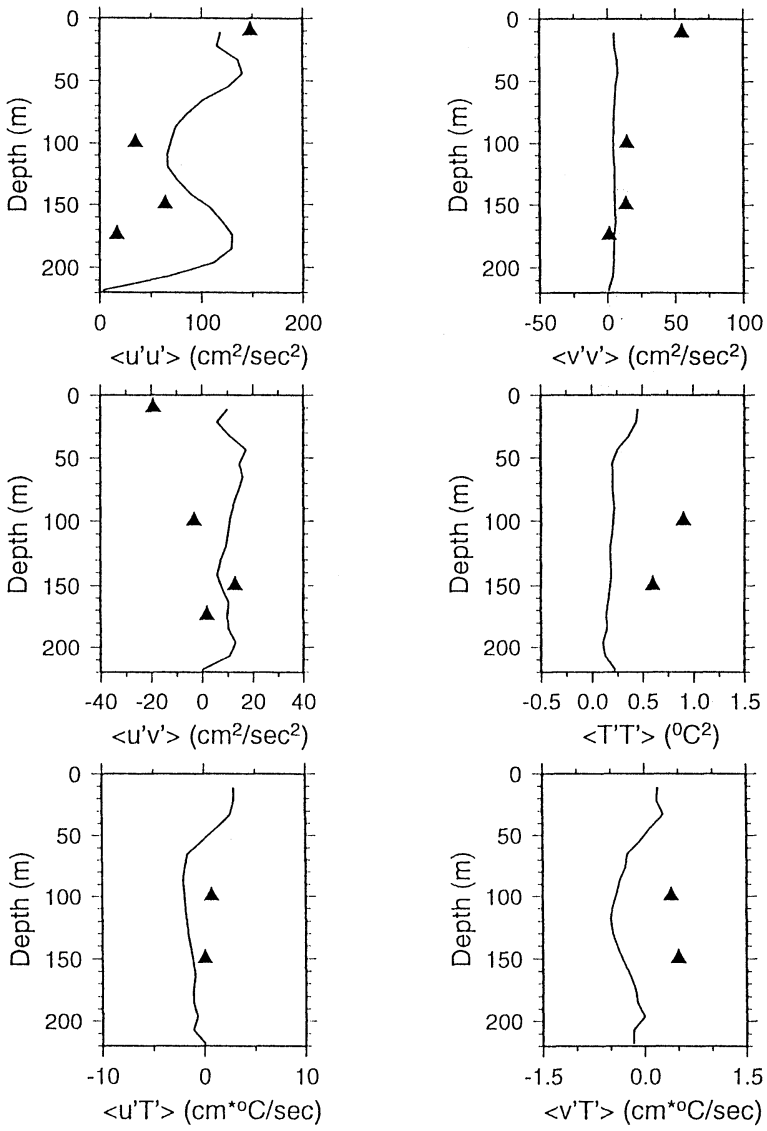

Fig. 11. Mean vertical profiles for Reynolds stress of model output (solid lines) and observed data (solid triangles). Upper-slope station (27.9°N; 210m water depth).

than in the observations. Also, there is a large variation in mean profiles between the outer-shelf (not shown) and upper-slope stations, a distance of ca. 40km, indicative of the need for higher spatial resolution in observations. Similarly, there is more vertical structure in the mean model flow profiles than the vertically sparse observations can define.

Spectrum analysis comparisons. The energy spectra for the model output (solid dots) and observed data (solid triangles), zonal and meridional velocity components are compared (Fig. 12). The Nyquist sampling frequency for the observed data is 1 cycle per hour, while for the model output it is 1 cycle per 10 days. As described earlier, the observed data were filtered and subsampled to a Nyquist sampling frequency of 4 cycles per day for autospectrum analyses (Fig.12); they were further filtered

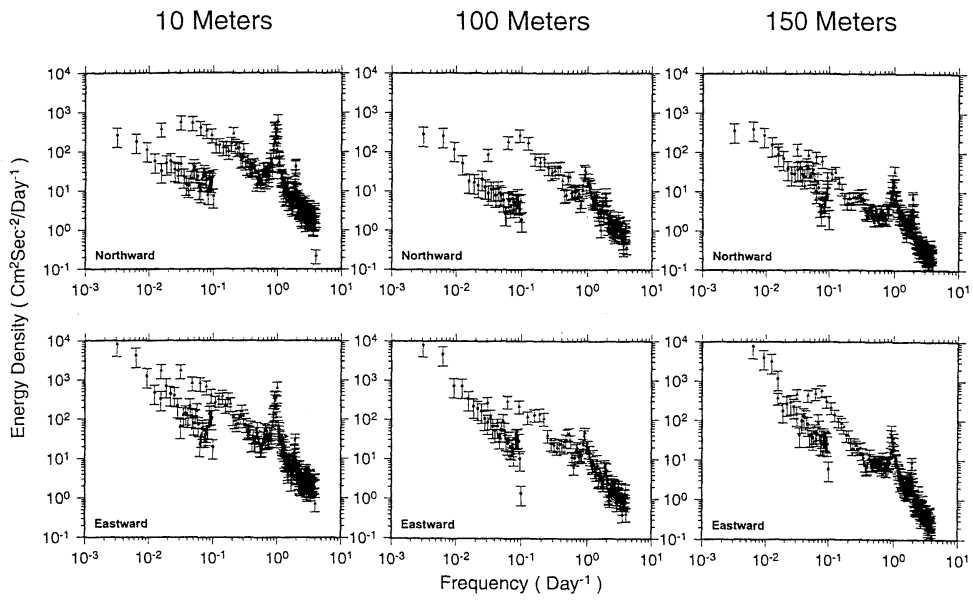

Fig. 12. Energy density spectra of model output (solid dots) and observed velocity data (solid triangles) and plus/minus standard deviation bars. Upper: meridional component; lower: zonal component; at upper-slope station (27.9°N; 210m water depth).

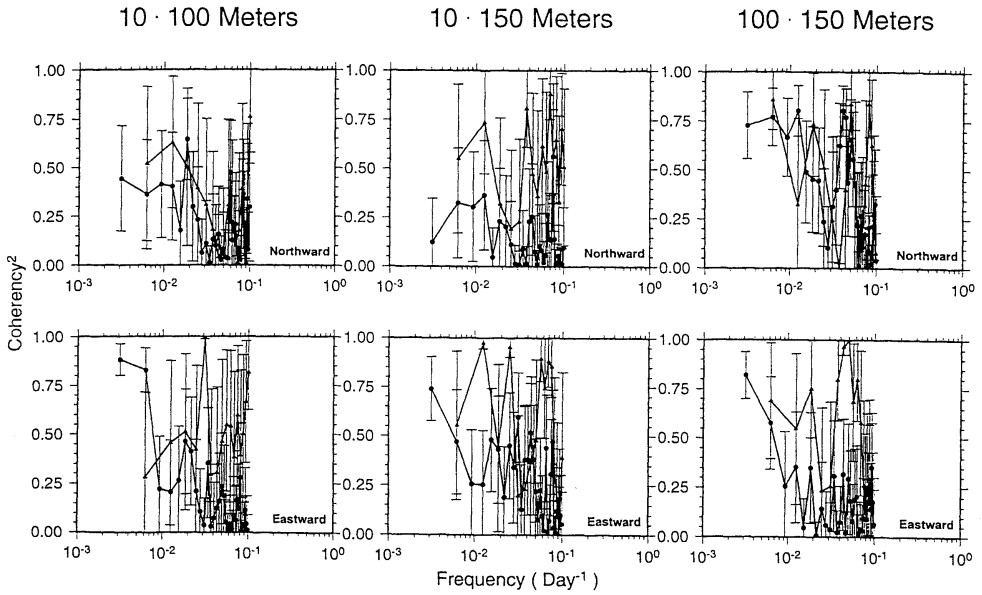

Fig. 13. Vertical coherence of model output (solid dots) and observed velocity data (solid triangles) and plus/minus standard deviation bars. Upper: meridional component; lower: zonal component; at upper-slope station (27.9°N; 210m water depth).

and subsampled to a Nyquist sampling frequency of 0.1 cycles per day for coherence analyses (Fig. 13). The lowest frequency resolved is 1 cycle per 100 days for the observed data and 1 cycle per 300 days for the model output. Standard deviation bars are shown for the ensemble-averaged spectra. As a consequence of the different sampling rates and record lengths,

the observed and model spectra only overlap in a spectral band between 0.02 and 0.1 cpd.

At the upper-slope station, there is an order of magnitude difference in energy levels at 10 and 100m, and even in the eastward component at 150m, in the 0.02 to 0.1 cpd spectral band. (Presumably, there may be better agreement when the model is forced with synoptic winds.) Overall, the energy level of the model output changes less with depth than does the energy level of the observed data. The spectra of observed data are a reminder that considerable energy exists at the diurnal-inertial (especially in the upper 10m), and some at the semidiurnal time scale which is not yet treated by the model. Similarly, there is considerable energy in the several-day band in the observed data which, if it existed in the model output, has been averaged out in the archival process. However, the energy in this band is likely generated by wind variations which the model could not reproduce at this stage due to the constant wind forcing.

The vertical coherence for the model output (solid dots) and of the observed data (solid triangles), zonal and meridional velocity components are compared (Fig.13). At the upper-slope station, the vertical coherence of the model output and observed data are, with a few exceptions, in qualitative agreement. For example, the vertical coherence generally decreases from time scales of 100 days to 30 days, but with a tendency for the observed values to rise near 10 to 20 days, probably reflecting the response to synoptic atmospheric forcing.

Overall, the observed spectra and vertical coherence results suggest that model results must account for the vigorous inertial and tidal motions over the Louisiana/Texas shelf, especially considering their probable importance to turbulent mixing.

5. Summary and conclusions

The Gulf of Mexico circulation model has means and variances which are commensurate with those of the observations on 92°W. However, there are important differences in detail. For example, the upper layer variance in the synoptic (spectral) band (3- to-10 days periods) is an order of magnitude less in the model output than in the observations. As another, the vertical coherence of the observed data considerably exceeds that of the model output in the 10- to -20 days band. The differences are probably mainly due to the model being forced by constant rather than synoptic winds.

Major features of the model output include two westward nearshore, nearsurface buoyant jets; an eastward shelfbreak, full-water-column zonal jet; and high variability at the shelfbreak, including that due to eddy passages. Strong patterns exist in model output fields over the continental slope, presumably due to eddy passages. Mean and variance fields from the model have coherent patterns on scales of 50 km horizontally and 50 m vertically. However, available observations lack sufficient resolution to validate such patterns.

The present results must be updated with results from improved model runs from the Gulf of Mexico Modeling Program, especially those runs with seasonal and synoptic atmospheric forcing, plus tidal forcing. They also need to be updated when more comprehensive observations become available from the LATEX field program. It will be important to archive at least portions of the model output at daily (or even hourly) intervals. The skill assessment methodology needs to be extended to include horizontal coherence, 3-D analyses, and diagnostics for dynamics and energetics.

Acknowledgements

This research is sponsored by the Minerals Management Service as part of the Gulf of Mexico Modeling Program under subcontract from Dynalysis of Princeton. It is also supported by the Ocean Pollution Research Center of the University of Miami under a bequest from the Brenauer Estate. Comments on a draft manuscript by Drs. Leo OEY, Rich PATCHEN, Fred VUKOVICH and Bill WISEMAN are highly appreciated.

References

BLUMBERG, A. F. and G. L. MELLOR (1983): Diagnostic and prognostic numerical circulation studies of the South Atlantic Bight. J. Geophys. Res., 88, 4579-4592.

COCHRANE, J. D. and F. J. KELLY (1986): Low frequency circulation on the Texas-Louisiana

continental shelf. J. Geophys. Res., **91**, 10645–10659.

HAMILTON, P. (1990): Deep currents in the Gulf of Mexico. J. Phys. Oceanogr., **20**, 1087–1104.

HAMILTON, P. (1992): Lower continental slope cyclonic eddies in the central Gulf of Mexico. J. Geophys. Res., **97**, 2185–2200.

HELLERMAN, S. and M. ROSENSTEIN (1983): Normal monthly wind stress over the world ocean with error estimates. J. Phys. Oceanogr., **13**, 1093–1104.

LEVITUS, S. (1982): Climatological atlas of the world ocean. NOAA Professional Pap. 13, NOAA, Rockville, Maryland, 173 pp.

National Geophysical Data Center (1986): World-wide gridded bathymetry–DBDB 5. Boulder, Colorado.

NOWLIN, W. D. and A. PARKER (1974): Effects of a cold-air outbreak on shelf water of the Gulf of Mexico, J. Phys. Oceanogr., **4**, 467–486.

OEY, L. -Y. and Y. -H. ZHANG (1993): Loop Current and eddies: model sensitivity experiments and analyses. Ocean Modeling Group Technical Report No. 15, Stevens Institute Tech., 37pp., 30 figs.